

Survey strategies to quantify and optimize detecting probability of a CO₂ seep in a varying marine environment



Hilde Kristine Hvidevold ^a, Guttorm Alendal ^{a,*}, Truls Johannessen ^b, Alfatih Ali ^a

^a Department of Mathematics, University of Bergen, Norway

^b Geophysical Institute, University of Bergen, Norway

ARTICLE INFO

Article history:

Received 17 April 2015

Received in revised form

12 May 2016

Accepted 7 June 2016

Available online 24 June 2016

Keywords:

Monitoring

Marine

Detection

Seeps

ABSTRACT

Designing a marine monitoring program that detects CO₂ leaks from subsea geological storage projects is challenging. The high variability of the environment may camouflage the anticipated anisotropic signal from a leak and there are a number of leak scenarios. Marine operations are also costly constraining the availability of measurements. A method based on heterogeneous leak scenarios and anisotropic predictions of chemical footprint under varying current conditions is presented. Through a cost function optimal placement of sensors can be given both for fixed installations and series of measurements during surveys. Ten fixed installations with an optimal layout is better than twenty placed successively at the locations with highest leakage probability. Hence, optimal localizations of installations offers cost reduction without compromising precision of a monitoring program, e.g. quantifying and reduce probabilities of false alarm under control. An optimal cruise plan for surveys, minimizing transit time and operational costs, can be achieved.

© 2016 The Authors. Published by Elsevier Ltd. This is an open access article under the CC BY license (<http://creativecommons.org/licenses/by/4.0/>).

1. Introduction

All geological CO₂ storage projects need a surface monitoring program with four main objectives; 1) maximize assurance of storage integrity, 2) assure that a leak will likely be detected, 3) continue to build an accurate baseline to capture trends and natural variability, and 4) to prevent unjustified accusations of adverse effects from the storage project (EU Commission, 2011; Blackford et al., 2015a). The 2011 incident at the Weyburn project is an example of the latter (Boyd et al., 2013).

With proper selection and operational procedures geological CO₂ storage projects will be designed not to leak. Geological monitoring of the reservoir, complex and overburden will be the primary monitoring strategy to assure operations according to plans and to detect any adverse events. Still, due to precision and resolution, there will always be an uncertainty that CO₂ migrates toward the surface undetected.

Transport of the CO₂ within the formation might find other potential pathways like fractures and/or faults or the CO₂ might create new pathways (Oldenburg and Lewicki, 2006). Leaks

following weakness zones in geological structures or old wells might cause high flux rates of CO₂ far away from the injection site. More diffusive leaks can be caused by CO₂ migrating through the overburden reaching the surface over a relatively large area. Leak scenarios will be an intrinsic component in site characterization and lay the ground for risk and impact assessments necessary for obtaining a permit.

The site specific spatial and temporal evolution of the CO₂ plume within the storage complex determines the area to be monitored. The anisotropic evolution of the Sleipner plume (see e.g. Boait et al. (2012)) illustrate that subsurface monitoring is a prerequisite for designing a marine monitoring program. For offshore storage projects a monitoring program for the seafloor and the water column can be costly, and the marine environment is hostile for instrumentations.

It is therefore suggested that the seafloor monitoring program has three levels of modus operandi; 1) anomaly detection modus, 2) confirmation and location modus, and 3) seep quantification modus. Blackford et al. (2015a) suggest a fourth step; impact assessment. All modes will have different needs with regards to instrumentation and data. As an example, location mode will require current predictions in real time to be able to move upstream from a signal, as opposed to the statistical current conditions that is sufficient for the detection modus.

* Corresponding author.

E-mail address: guttorm.alendal@uib.no (G. Alendal).

The focus here is the detection phase, in which the monitoring program looks for anomalies in the environment. How can a potential seep be detected, and is it possible to quantify the certainty of detecting a leak? Answering these questions relies on 1) where will a leak most likely occur, 2) how will a seep trail materialize in the water column, and 3) will it be possible to distinguish the signal from the background variability?

Leak of CO₂ shallower than 500 m will rise in the water column as gas bubbles (Alendal and Drange, 2001). Depending on the flux rate, it might create individual bubbles, bubble trains or bubble plumes. The dynamics of these regimes are different, with the plume dynamics being the most challenging to model due to the two way coupling with the surrounding seawater.

In all cases an increase in CO₂ concentration is expected in the vicinity of a leak, with subsequent possible environmental impacts (Blackford et al., 2010). The spatial extent of area influenced is expected to be limited (Dewar et al., 2013, 2014), but might become severe depending on the size of the leakage flux and the dilution rate in the water column.

Environmental changes might serve as indicators that a leak is occurring, either through changes in bottom fauna or in the pelagic ecosystem, and detection of bubbles can be made from ship sonars (Brewer et al., 2006; Noble et al., 2012). In addition the elevated concentration of dissolved CO₂ can be used as indicators of a leak.

One main challenge will be to define the degree of anomaly needed in order to mobilize the more expensive confirmation and localization step, balancing the need for confirmation with the cost of false alarms. Changes in flux or new occurrences of natural gas seeps, changes in biota or CO₂ concentration can only be distinguished if a proper baseline statistic is available.

In the present study elevated CO₂ concentrations is used as the methodology to design a monitoring program. CO₂ is naturally present as dissolved into seawater and an increase of CO₂ concentration is expected according to the acidification of marine waters (Caldeira and Wickett, 2003). Botnen et al. (2015) demonstrated a stoichiometric approach for detection of small CO₂ concentrations that might stem from seeps, lowering the concentration threshold for a signal to become statistically significant. This method lies in between the statistical power analysis for obtaining an environmental baseline (Yang et al., 2011a) and the pure process based monitoring approach suggested by Romanak et al. (2012).

The marine waters are in constant motion and are characterized with high variability; Tides change current directions, wind alters the amount of mixing, and local topography change local current conditions (Alendal et al., 2005). Footprints of leaks are thus a varying and highly anisotropic signal depending strongly on the local oceanic and atmospheric conditions (Alendal et al., 2013; Greenwood et al., 2015; Ali et al., 2016). This makes designing a monitoring framework considerably harder compared to when assuming isotropic signal (Yang et al., 2011b).

Hvidevold et al. (2015) presented a procedure for optimizing the sensor placement on the seafloor that partly accounts for footprint anisotropy. The highly anisotropic footprint signal prediction from a General Circulation model (Alendal et al., 2013; Ali et al., 2016) was simplified through a least square approximation to an ellipsoid, generating orthogonal major and minor directions. It was observed that this procedure reduced the area of detectable concentration compared to the average field itself.

In this study the same GCM simulations is used and a method to use the predicted footprints directly is introduced. This method combined with predicted time-series in an array of 51 × 51 grid points around the seep location open for other approaches in designing a monitoring program. Three different methods will be presented; i) an average method to compare with results from the previous study (Hvidevold et al., 2015), ii) an event method taking

into account the occasionally elevated concentrations and iii) a single measurement method. The two former represent fixed installations, with different approach in data analysis, while the latter can represent measurements taken during cruises and surveys.

By combining the stoichiometric approach in (Botnen et al., 2015) and the statistical approach suggested has the potential to become a powerful tool to discover small leaks from CCS. Such leaks matters on an environmental scale and may become harmful for the environment and contribute to ocean acidification. Very small natural CO₂ leaks from the Jan Mayen fracture zone is proven to be discovered by using the stoichiometric approach (Botnen et al., 2015). Here the focus is to arrive to the optimal placement of sensors on the sea floor to obtain an early detection of a potential leak from subsea geological storage of CO₂.

2. Problem definition

It is not the scope to perform a detailed site specific design, nor is a proper assessment of possible leakage pathways available for candidate CCS storage sites. Hence, in this study a synthetic area of 31 × 31 km containing 16 randomly placed wells is used. In reality geological weakness zones needs to be included as well.

Since CO₂ might also migrate in the lateral direction during ascent, the seep is assumed to have a probability of surfacing a distance from the well, located in \mathbf{x}_1 , according to

$$p(\mathbf{x}) = p_0 \exp \left[- \left(\frac{\mathbf{x} - \mathbf{x}_1}{\sigma} \right)^2 \right], \quad \mathbf{x} \in \mathbf{R}^2. \quad (1)$$

The value p_0 is the probability of leakage through the well and σ describes how quickly this probability levels off. It is assumed that all wells have the same p_0 and $\sigma \approx 0.6$ km. This is a simplification, in reality some wells may reach the storage formation and some will not.

To account for potential unknown pathways a low background probability is added to the map, assuming a ~10 times higher probability for leakage in a well compared to the background. Under the assumption that a leak is ongoing within the area probability field is normalized i.e., the probability that a leak occurs is 1.

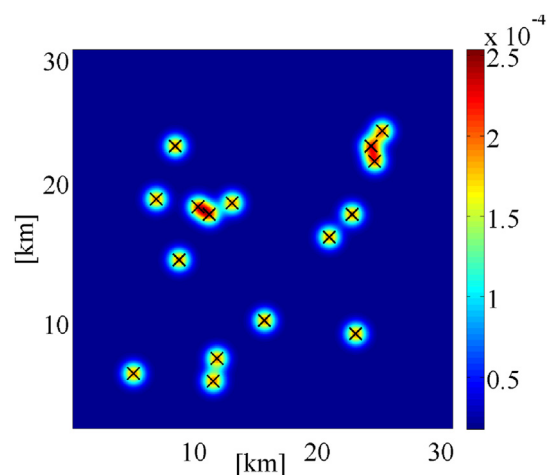


Fig. 1. The many pathways to the surface, either already present or mobilized by the storage project, needs to be identified and leak scenarios defined. In the present study a synthetic map defining areas of probable leak locations is used. In a (31 × 31) km synthetic area of the seafloor over a storage site a number of well locations are represented by black crosses. Under the assumption that a leak is ongoing. The colors indicates the probability of being the location of the seep. (For interpretation of the references to colour in this figure legend, the reader is referred to the web version of this article.)

Fig. 1 shows the resulting probabilities.

Simulating a seep is challenging, especially due to the many different scales that are involved, ranging from 10^{-2} m (bubble scale) to $10^2 - 10^3$ m (scale of dynamically active concentration field) (Alendal and Drange, 2001; Sato and Sato, 2002; Dewar et al., 2013, 2014). Away from the dynamically active seep zone the CO_2 concentration behaves as a passive tracer, being transported and further mixed by local currents and turbulence. Locally there might be strong variations in current conditions and mixing, influenced by a number of factors such as surface wind, tide (Davies and Furnes, 1980) and topography (Alendal et al., 2005).

To obtain a footprint a 800 m resolution regional ocean model (Bergen Ocean Model; BOM) set-up for the North Sea advects and disperse CO_2 as a passive tracer (Alendal et al., 2013; Ali et al., 2016). The model forcing comprises tide (Davies and Furnes, 1980) (4 tidal constituents; M_2 , S_2 , K_1 , and N_2), river runoff data, and initial and lateral boundary conditions for salinity and temperature taken from the UK Metoffice FOAM 7 km model published at (<http://www.myocean.eu/>). The atmospheric forcing is based on spring 2012 data, collected and interpolated from The European Centre for Medium-Range Weather Forecasts (ECMWF, the Centre). In the vertical 41 sigma-coordinate layers is used, distributed with higher resolution (1 m) near the free surface and the sea floor. In this study a source term representing a leak rate of 1.74 kg/s, with a flux area representing one grid cell of (800×800) m² located closest to the seabed, i.e. the grid-cell closest to the seafloor.

A two months simulation of CO_2 seep has been used to gather time series, with 1 min resolution, in a 51×51 grid cell array in the vicinity of the leakage. Fig. 2 show time series for nine grid cells closest to the leakage point (blue lines).

The reported precision for measurements of total inorganic carbon (c_t) is $\sim 0.090 \cdot 10^{-3}$ kg/m³ (Dickson et al., 2007), shown as green line in Fig. 2. In the North Sea the natural variability of c_t between seasons varies between $2.260 \cdot 10^{-3}$ kg/m³ and $4.520 \cdot 10^{-3}$ kg/m³ mainly caused by e.g. changes in biological processes (photosyntheses and respiration), air-sea exchange, and hydrography (salinity variations and mixing between watermasses) (Omar et al., 2005; Salt et al., 2013).

Omar et al. (2005) and Botnen et al. (2015) developed a

conceptual model correcting for the natural variability and the anthropogenic trend based upon a stoichiometric approach. When contrasting measurements with a reference location it is possible to determine changes in c_t that must stem from other sources, like seeps of CO_2 . The threshold for detecting anomalies after applying this conceptual model is $c_t = 0.226 \cdot 10^{-3}$ kg/m³ (red lines in Fig. 2). The different concentration lines in Fig. 2 clearly illustrate the threshold reduction offered.

As a further simplification the constant leakage rate and the resulting seafloor concentration are independent on leak location. In reality flux will be dependent on leak location and be time dependent, and local topography and current variability might alter the characteristics. For a better description seasonal, spatial variability and long term trends will have to be accounted for. This will require availability of the aforementioned current statistics and a much more comprehensive simulation study.

3. Monitoring design

The main challenge is how and where to do measurements with the purpose of detecting a leak. Based on the GCM time series predictions, three different approaches is presented. Each building on a detection probability function, $G(\mathbf{x} - \mathbf{x}_l; c_t)$, that gives the probability of detecting a leak at \mathbf{x}_l if a measurement is taken at \mathbf{x} and with a given a detection threshold c_t .

3.1. Three strategies for detecting a leak

3.1.1. The average concentration method

This method uses the average CO_2 concentration, $\bar{C}(\mathbf{x})$, collected at fixed locations, hence represent instrumentations deployed at fixed locations over a period of time. The detection probability function is defined

$$G_A(\mathbf{x}; c_t) = \begin{cases} 1 & \text{if } \bar{C}(\mathbf{x}) > C_t \\ 0 & \text{elsewhere} \end{cases} \quad (2)$$

Fig. 3) shows the average concentration, $\bar{C}(\mathbf{x})$, for all 51×51 grid cells. $G(\mathbf{x})$ have the value 1 if the average CO_2 concentration is above the threshold concentration c_t , i.e. inside the blue contour in Fig. 3),

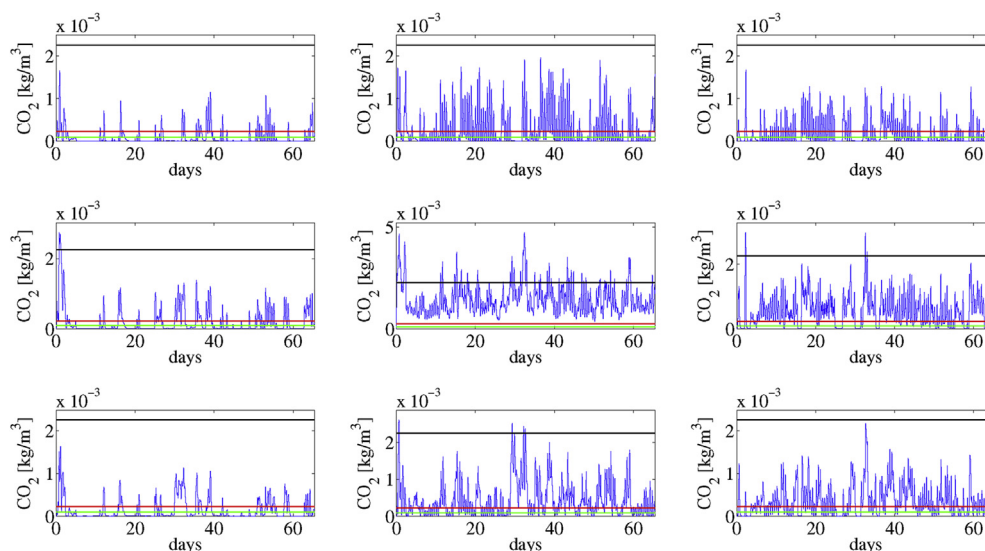


Fig. 2. The time series for the anisotropic CO_2 signal along the seafloor for a leakage point (in the middle), and the 8 grid cells surrounding it. The blue lines show the concentration for each time step in the grid cell, the red lines show the threshold concentration if environmental baseline is available ($c_t = 0.226 \times 10^{-3}$ kg/m³). The black horizontal lines show the detection threshold if baseline statistics is not available ($2.26 \cdot 10^{-3}$ kg/m³). The green line shows instrument accuracy ($0.090 \cdot 10^{-3}$). Note the different scaling on the y axis. (For interpretation of the references to colour in this figure legend, the reader is referred to the web version of this article.)

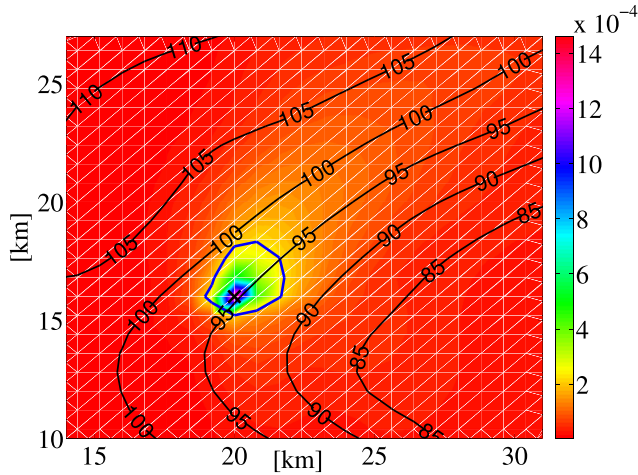


Fig. 3. Simulated average CO₂ concentration in the vicinity leakage, the threshold $c_t = 0.226 \times 10^{-3} \text{ kg/m}^3$ is shown by the blue contour line. The black contour lines represent the bathymetry in meter illustrating the role of topography in determining the principal directions of the signal. (For interpretation of the references to colour in this figure legend, the reader is referred to the web version of this article.)

and zero on the outside.

In Hvidevold et al. (2015) this footprint was used to approximate an analytical function, introducing additional approaches and simplifications to the problem. Here the simulated footprint is used directly. In reality this method will not be used, it is shown here for comparison with the previous study (Hvidevold et al., 2015). To wait until the average concentration becomes statistically significant will delay the detection, or even prevent, the leak to be detected.

3.1.2. Single measurement method

In the single measurement method the time series predictions are used to calculate the relative time the concentration is above the threshold concentration, c_t . The probability, $G_S(\mathbf{x}; c_t)$, is formed by counting the data points above c_t divided by the total amount of data, i.e. a frequentist approach,

$$G_S(\mathbf{x}; c_t) = \frac{\sum_{l=1}^k f(C_l(\mathbf{x}; c_t))}{k} \quad \text{where} \quad f(C_l(\mathbf{x}; c_t)) = \begin{cases} 1 & \text{if } C_l(\mathbf{x}) > c_t \\ 0 & \text{elsewhere} \end{cases} \quad (3)$$

where k is the number of equidistant data points in the time series.

Rephrased, the function gives the probability of a single measurement at \mathbf{x} to be above c_t . For instance in the grid cell located at the leakage point, the center plot in Fig. 2, the concentration is always above the threshold concentration $c_t = 0.226 \times 10^{-3} \text{ kg/m}^3$, hence $G(\mathbf{x}; c_t) = 1$. While in the lower left plot the concentration is often below this c_t and the probability for a single measurement to detect the leak is 0.23. Calculating $G_S(\mathbf{x}; c_t)$ for all 51×51 grid cells gives a probability field around the leakage, Fig. 4.

3.1.3. Event based method

This represent a combination of the two former approaches, continuous measurements at fixed locations and utilizing $G_S(\mathbf{x}; c_t)$. A fixed installation might experience periods of increased CO₂.

If p is the relative time the concentration is above c_t , contours of constant $G_S(\mathbf{x}; c_t) = p$ represent the boundary for areas with higher frequency of CO₂ concentration above the detection threshold. To avoid that outliers cause false alarms the concentration should be above the threshold concentration a given fraction of

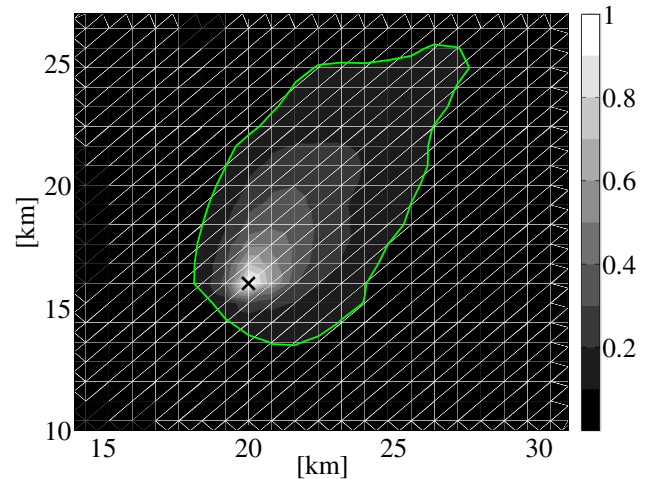


Fig. 4. The probability for the footprint to be above the $C > 0.226 \times 10^{-3} \text{ kg/m}^3$ threshold at any time in the vicinity of the leakage represented by the black cross. The green contour line represent 0.1, so any measurements taken inside of this contour will have 10% probability of being above the detection threshold at a given time. (For interpretation of the references to colour in this figure legend, the reader is referred to the web version of this article.)

the time p_t . Hence this method uses the probability function

$$G_E(\mathbf{x}; c_t, p_t) = \begin{cases} 1 & \text{if } G_S(\mathbf{x}; c_t) > p_t \\ 0 & \text{elsewhere.} \end{cases} \quad (4)$$

The green contour line in Fig. 4 represent $p_t = 0.1$, bounding the area for which a sensor can detect a leak $G_E(\mathbf{x}; c_t, p_t) = 1$.

3.2. Designing the optimal monitoring system

All three approaches use the assumption that a leak is occurring within the area shown in Fig. 1 and the predicted CO₂ concentration footprint time series, exemplified in Fig. 2, is independent of leak location. One problem is to invert the probability functions defined to the area monitored by a measurement taken at a given location.

Given a measurement at a fixed \mathbf{x}_a , the probability of detecting a leak at \mathbf{x}_l will be $G(\mathbf{x}_a - \mathbf{x}_l; c_t)$, where G is any of the probability functions defined earlier. Treating \mathbf{x}_l as the independent variable the probability fields of detecting a leak at $\mathbf{r} = \mathbf{x} - \mathbf{x}_a$ will be $G(-\mathbf{r}; c_t)$, representing a 180° rotation of the anisotropic G contours. If measurements taken at \mathbf{x}_a show no indications of a leak the leak probability map can be updated this new information.

Fig. 5 illustrates this for a single measurement point in a section of the leak probability map, Fig. 1. The probability of any coordinates being the site of a leak prior to any measurements (a) is updated with the new belief after measuring no indication of a leak at \mathbf{x}_a , white cross, for the different methods. The average method (b) and the event method (d) rule out a leak in the area monitored, with the area monitored by the average method being considerably smaller. If a single measurement stays below the threshold concentration a leak can not be ruled out completely, but the probability map may be updated by subtracting $G(-(\mathbf{x} - \mathbf{x}_a); c_t)$ as shown in Fig. 5(c).

The design problem is to localize where to take n measurements in an optimal way. For instance, placing a measurement in a location already covered will give low use of that measurement. This is solved using Matlab's built-in genetic algorithm, *ga*, with a population size of 300 individuals (collections of measurement coordinates). The genetic algorithm will evolve the population of measurement collections toward higher probable detection. The

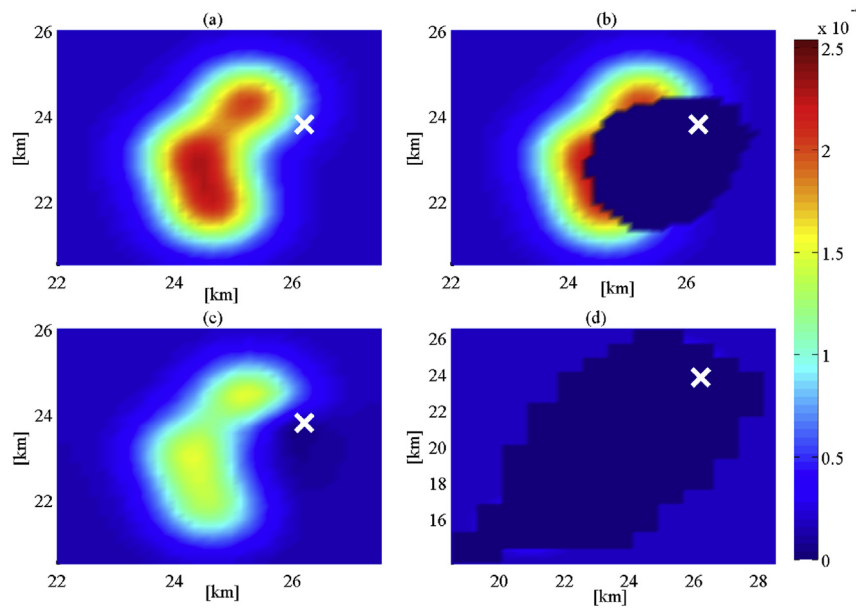


Fig. 5. Illustrating the methods by one measurement in a section of the probability map Fig. 1. Upper left (a) show the location of a measurement and the local probability of being the location of the leak. The remaining subfigure shows the monitored area of measuring at the white cross for (b) the average method, (c) the single method and (d) the event method. Note that Fig. (d) shows a larger spacial area than (a), (b) and (c).

benefit of this method is the global search space offered, avoiding getting trapped in local optimums.

4. Results

Fig. 6 show the probability to detect a leakage as function of number of measurements for the different methods, demonstrating the ability of the procedure to quantify the leak detection capability of a measurement grid.

The average method is very conservative in the sense that average concentration must become statistically significant before a leakage is detected. In reality a fixed installation will detect a leakage immediate once the measurements becomes significantly different from the natural variability. This is also illustrated by the small area covered in Fig. 5(b).

Fig. 6 also show that fixed installations (event) gives much higher detection probability than single measurements, given similar amount of measurements. For instance placing 2 fixed installations is better than taking 7 single measurements, and

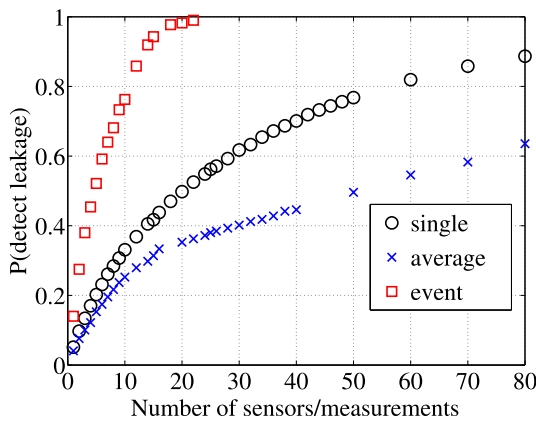


Fig. 6. The probability of detecting a leakage as function of number of measurements, using detection threshold $c_t = 0.226 \cdot 10^{-3} \text{ kg/m}^3$.

requiring a detection probability of 80% only 12 fixed installations is needed compared to 60 single measurements. This is due to the fact that fixed installations represent many measurements taken at the same position, and hence increase the probability of capture periods of elevated CO₂ concentrations. Due to logistics and cost it might still be beneficial to rely on cruises and taking point measurements and the method has the ability to locate where these should be taken.

Due to the many simplifications and assumptions made the numerical values should be used with caution. Still it is interesting to see how much better an optimal layout of measurements will perform compared to an intuitive approach with successively selecting locations based on highest remaining probability of leaks, Table 1. For instance, the event based method using 10 locations with an optimal layout is much better than using 20 measurements with the intuitive layout.

The optimal layout for the three methods, using four and ten

Table 1

The probability to detect leakage using optimal layout, column 3, and intuitive layout by selecting successively the location with highest probability of being the location of the leak, column 4. Column 1 gives number of measurements and the detection method is shown in column 2.

Measurements	Method	Optimal [%]	Intuitive [%]
2	Event	27.5	24.0
4	Event	45.4	33.2
10	Event	76.3	60.8
15	Event	94.3	64.9
20	Event	98.2	70.5
2	Single	9.7	9.1
4	Single	17.0	13.8
10	Single	33.1	30.8
15	Single	40.7	41.7
20	Single	61.7	48.0
2	Average	7.6	5.8
4	Average	12.2	10.9
10	Average	25.3	22.5
15	Average	31.4	29.7
20	Average	35.3	32.1

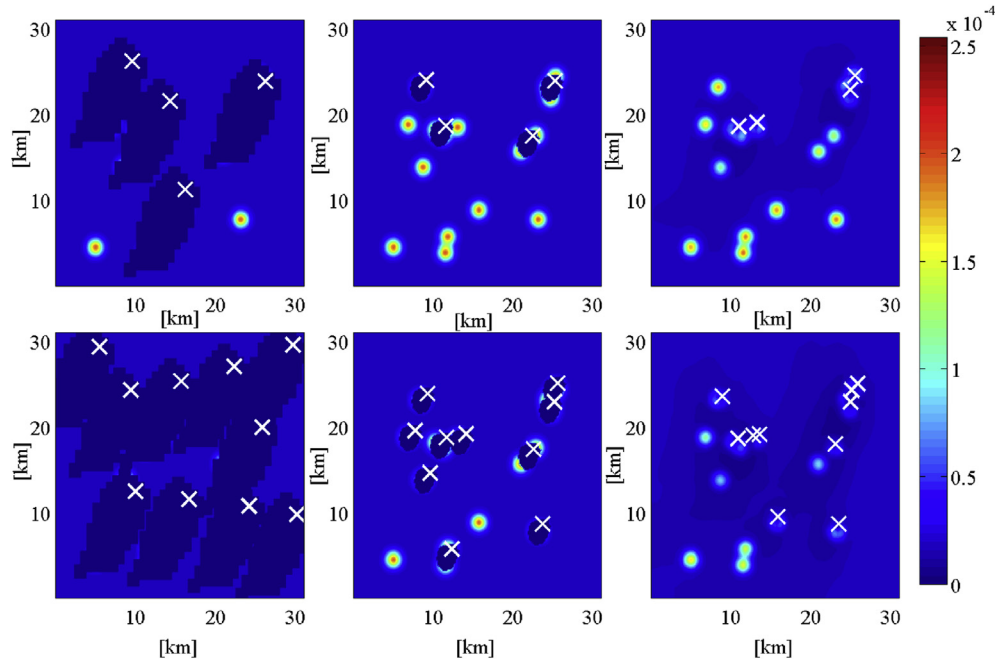


Fig. 7. Optimal layout for 4 measurements, top row, and 10 measurements, bottom row. In the left most figures the event based method is used, in the middle column the average method is used and to the right side single measurement method is used. The white crosses show the action location.

measurements, is shown in Fig. 7. For the average method the area covered by the measurement is almost as big as the leakage probability area surrounding a well, and the optimal layout is to cover a new well location for each new measurement, therefore it is almost similar to the intuitive strategy as can also be read from Table 1.

One measurement can cover several wells if the event based method is used. Therefore it is not necessarily optimal to place measurements directly on well locations. Single measurement method require clustering of measurements in order to optimize detection. In addition the preferred location is downstream due to the anisotropy seen in Fig. 4.

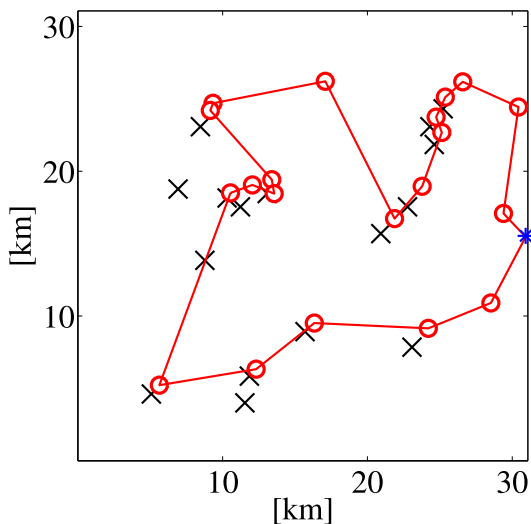


Fig. 8. The shortest travel route when taking measurements after optimal layout for twenty locations, red circles. Minimum travel distance is 99 km, using the same start and the end location blue star. The black crosses show the well locations. (For interpretation of the references to colour in this figure legend, the reader is referred to the web version of this article.)

5. Discussion

The results presented here are based on many simplifications and short cuts due to lack of information and data. Still it is demonstrated that combining proper site characterization, environmental baseline statistics and leak footprint predictions can be combined to optimize the required marine monitoring program.

At the moment the necessary information to perform a real design at a real site is lacking and hence the possibility of demonstrating the concept in-situ. To perform a more comprehensive design for a future storage project will require a thorough geological survey identifying potential leakage pathways, including mutual propensity to leak, to get a more realistic probability map (Fig. 1). In addition a proper environmental baseline is needed for better detection limit, as part of this baseline spatial and temporal current statistics should be gathered for reliable footprint prediction.

The aim must be to get involved in future storage demonstration projects with the purpose of assuring that necessary information is gathered during site characterization and selection. However, these demonstration storage sites will be designed to not leak and cannot be used to test the concept. Such test will require in-situ experiments, like the QICS experiment (Blackford et al., 2015b), or use of natural gas seeps. In any case it will require resources that are not available for the moment.

Higher confidence in the monitoring program is achieved through quantification of the degree of certainty when a leak is indicated. Such indication will mobilize extra resources to confirm and localize a potential leak. The operations might become costly and false alarms should be avoided. On the other hand it is necessary to act on indicators of leaks in order to identify and mitigate impacts. Through the certainty quantification offered by the method suggested here it is possible to judge the likelihood of an indication being a false alarm.

Cost for operation and installation has not been considered in this study. Assuming the optimal measurement layout has been chosen, minimizing the travel distance between these locations

will save time and cost. This will be true for installations requiring ships, operating gliders or other new technologies. This is exemplified in Fig. 8 show the shortest travel route for the single measurement methods for twenty locations, using the same start and stop location, blue star, using the genetic algorithm.

Acknowledgement

This work has been funded by SUCCESS centre for CO₂ storage under grant 193825/S60 and the CLIMIT program under grant 254711/E20 from Research Council of Norway (RCN). In addition, the research leading to these results has received funding from the European Community's Seventh Framework Programme (FP7/2007–2013) under grant agreement no [265847].

References

- Alendal, G., Berntsen, J., Engum, E., Furnes, G.K., Kleiven, G., Eide, L.L., 2005. Influence from 'ocean weather' on near seabed currents and events at Ormen Lange. *Mar. Pet. Geol.* 22 (1), 21–31.
- Alendal, G., Dewar, M., Ali, A., Evgeniy, Y., Vielstädte, L., Avlesen, H., Chen, B., 2013. Technical Report on Environmental Conditions and Possible Leak Scenarios in the North Sea. Tech. Rep. D3.4, ECO2 deliverables. <http://www.eco2-project.eu>.
- Alendal, G., Drange, H., 2001. Two-phase, near-field modeling of purposefully released CO₂ in the ocean. *J. Geophys. Res.* 106 (C1).
- Ali, A., Frøysa, H.G., Avlesen, H., Alendal, G., Jan. 2016. Simulating spatial and temporal varying CO₂ signals from sources at the seafloor to help designing risk-based monitoring programs. *J. Geophys. Res.-Oceans* 121 (1), 745–757.
- Blackford, J., Bull, J.M., Cevatoglu, M., Connelly, D., Hauton, C., James, R.H., Lichtschlag, A., Stahl, H., Widdicombe, S., Wright, I.C., Jul. 2015a. Marine baseline and monitoring strategies for Carbon Dioxide Capture and Storage (CCS). *Int. J. Greenh. Gas Control* 38, 221–229.
- Blackford, J., Stahl, H., Kita, J., Sato, T., Jul. 2015b. Preface to the QICS special issue. *Int. J. Greenh. Gas Control* 38, 1–1.
- Blackford, J.C., Widdicombe, S., Lowe, D., Chen, B., Sep. 2010. Environmental risks and performance assessment of carbon dioxide (CO₂) leakage in marine ecosystems. In: *Developments and Innovation in Carbon Dioxide (CO₂) Capture and Storage Technology, Volume 2-Carbon Dioxide (CO₂) Storage and Utilisation*. Woodhead Publishing Limited, pp. 344–373.
- Boait, F.C., White, N.J., Bickle, M.J., Chadwick, R.A., Neufeld, J.A., Huppert, H.E., Mar. 2012. Spatial and temporal evolution of injected CO₂ at the Sleipner field, North Sea. *J. Geophys. Res. Solid Earth* (1978–2012) 117 (B3).
- Botnen, H., Omar, A., Thorseth, I., Johannessen, T., Alendal, G., 2015. The effect of submarine CO₂ vents on seawater: implications for detection of subsea carbon sequestration leakage. *Limnol. Oceanogr.* 60 (2).
- Boyd, A.D., Liu, Y., Stephens, J.C., Wilson, E.J., Pollak, M., Peterson, T.R., Einsiedel, E., Meadowcroft, J., May 2013. Controversy in technology innovation: contrasting media and expert risk perceptions of the alleged leakage at the Weyburn carbon dioxide storage demonstration project. *Int. J. Greenh. Gas Control* 14, 259–269.
- Brewer, P.G., Chen, B., Warzinski, R., Baggeroer, A., Peltzer, E.T., Dunk, R.M., Walz, P., Dec 2006. Three-dimensional acoustic monitoring and modeling of a deep-sea CO₂ droplet cloud. *Geophys. Res. Lett.* 33 (23), 5.
- Caldeira, K., Wickett, M.E., 2003. Oceanography: anthropogenic carbon and ocean pH. *Nature* 425 (6956), 365–365.
- Davies, A.M., Furnes, G.K., 1980. Observed and computed M₂ tidal currents in the North Sea. *J. Phys. Oceanogr.* 10 (2), 237–257.
- Dewar, M., Sellami, N., Chen, B., 2014. Dynamics of rising CO₂ bubble plumes in the QICS field experiment. *Int. J. Greenh. Gas Control*. <http://dx.doi.org/10.1016/j.ijggc.2014.11.003>.
- Dewar, M., Wei, W., McNeil, D., Chen, B., 2013. Small-scale modelling of the physiochemical impacts of CO₂ leaked from sub-seabed reservoirs or pipelines within the North Sea and surrounding waters. *Mar. Pollut. Bull.* 73, 504–515. <http://dx.doi.org/10.1016/j.marpolbul.2013.03.005>.
- Dickson, A., Sabine, C., Christian, J.E., 2007. Guide to Best Practices for Ocean CO₂ Measurements. PICES Special Publication 3.
- EU Commission, 2011. Implementation of Directive 2009/31/EC on the Geological Storage of Carbon Dioxide, CO₂ Storage Life Cycle Risk Management Framework. Guidance Document 2.
- Greenwood, J., Craig, P., Hardman-Mountford, N., Aug. 2015. Coastal monitoring strategy for geochemical detection of fugitive CO₂ seeps from the seabed. *Int. J. Greenh. Gas Control* 39, 74–78.
- Hvidevold, H.K., Alendal, G., Johannessen, T., Ali, A., Mannseth, T., Avlesen, H., 2015. Layout of CCS monitoring infrastructure with highest probability of detecting a footprint of a CO₂ leak in a varying marine environment. *Int. J. Greenh. Gas Control* 37, 274–279.
- Noble, R.R.P., Stalker, L., Wakelin, S.A., Pejčić, B., Leybourne, M.I., Hortle, A.L., Michael, K., Sep 2012. Biological monitoring for carbon capture and storage – a review and potential future developments. *Int. J. Greenh. Gas Control* 10, 520–535.
- Oldenburg, C.M., Lewicki, J.L., 2006. On leakage and seepage of CO₂ from geologic storage sites into surface water. *Environ. Geol.* 50 (5), 691–705.
- Omar, A., Johannessen, T., Bellerby, R.G., Olsen, A., Anderson, L.G., Kivimäe, C., 2005. Sea ice and brine formation in Storfjorden: implications for the Arctic winter time air-sea CO₂ flux. In: *The Nordic Seas: an Integrated Perspective*, pp. 177–187.
- Romanak, K.D., Bennett, P.C., Yang, C., Hovorka, S.D., Aug. 2012. Process-based approach to CO₂ leakage detection by vadose zone gas monitoring at geologic CO₂ storage sites. *Geophys. Res. Lett.* 39 (15).
- Salt, L.A., Thomas, H., Prowe, A., Borges, A.V., Bozec, Y., Baar, H.J., 2013. Variability of North Sea pH and CO₂ in response to North Atlantic oscillation forcing. *J. Geophys. Res. Biogeosci.* 118 (2), 1584–1592.
- Sato, T., Sato, K., 2002. Numerical prediction of the dilution process and its biological impacts in CO₂ ocean sequestration. *J. Mar. Sci. Technol.* 6 (4), 169–180.
- Yang, Y.-M., Small, M.J., Junker, B., Bromhal, G.S., Strazisar, B., Wells, A., Oct. 2011a. Bayesian hierarchical models for soil CO₂ flux and leak detection at geologic sequestration sites. *Environ. Earth Sci.* 64 (3), 787–798.
- Yang, Y.-M., Small, M.J., Ogretim, E.O., Gray, D.D., Bromhal, G.S., Strazisar, B.R., Wells, A.W., 2011b. Probabilistic design of a near-surface CO₂ leak detection system. *Environ. Sci. Technol.* 45 (15), 6380–6387.